

CENTERIS 2014 - Conference on ENTERprise Information Systems / ProjMAN 2014 -  
International Conference on Project MANAGEMENT / HCIST 2014 - International Conference on  
Health and Social Care Information Systems and Technologies

## PS-InSAR monitoring of landslide activity in the Black Sea coast of the Caucasus

Elena Kiseleva<sup>a</sup>, Valentin Mikhailov<sup>a</sup>, Ekaterina Smolyaninova<sup>a</sup>, Pavel Dmitriev<sup>a</sup>,  
Vasily Golubev<sup>a</sup>, Elena Timoshkina<sup>a</sup>, A. Hooper<sup>b</sup>, S. Samiei-Esfahany<sup>c</sup>, R. Hanssen<sup>c</sup>

<sup>a</sup> *Schmidt Institute of physics of the Earth, Russian academy of Sciences, 10 B. Gruzinskaya, 123995, Moscow, e.kiseleva@ifz.ru*

<sup>b</sup> *School of Earth and Environment, University of Leeds, Leeds, LS2 9JT, A.Hooper@leeds.ac.uk*

<sup>c</sup> *Delft University of Technology, Delft, Stevinweg 1, 2628 CN Delft, NL, The Netherlands. R.F.Hanssen@tudelft.nl*

---

### Abstract

The landslide activity in the area of Bolshoy Sochi (Big Sochi) situated at the Black Sea coast of the Great Caucasus has been studied using the StaMPS PS-InSAR method. We incorporated three sets of radar images from the satellites with different wavelengths ALOS, Envisat and Terra-SAR-X from both ascending and descending tracks which cover the time period from January 2007 to September 2012. Comparative investigation of surface displacements obtained from all the data sets is presented. Areas where high surface displacement rates have been located on the base of the satellite data coincide well with zones of high landslide activity according to ground observations. We constructed time series for the two landslides: in the Baranovka and Mamaika villages where considerable surface movements had been observed during the time of acquisitions. Analysis of the time series made it possible to determine periods of activity and relative stability of the landslides and compare them with ground observations.

© 2014 The Authors. Published by Elsevier Ltd. This is an open access article under the CC BY-NC-ND license (<http://creativecommons.org/licenses/by-nc-nd/3.0/>).

Peer-review under responsibility of the Organizing Committee of CENTERIS 2014.

*Keywords:* PS-InSAR; StaMPS; landslides; Great Caucasus; comparison to ground data.

---

### 1. Introduction

The Black Sea coast of the Great Caucasus has always been a region of high landslide risk due to widely spread clays and marls seasonally saturated by abundant rainfalls. In recent years landslide risk assessment has become vital because of strongly increasing human-induced impact dealt with the Sochi-2014 Olympic Games. Methods of

synthetic aperture radar (SAR) interferometry proved to be a powerful tool while investigating ground movements within large territories. To estimate ground displacements, a pair of SAR images of a study area from the same track is processed to form an interferogram which shows phase shift of the reflected signal between acquisitions wrapped by modulo  $2\pi$ . The unwrapping procedure is used to transform these phase shifts to the surface displacements. Temporal changes of scattering properties of the Earth's surface and look angle direction reduce the efficiency of SAR interferometry. Besides, the signal due to displacement of the ground reflectors is often overprinted by atmospheric noise and artefacts caused by inaccuracy of satellite orbit and digital elevation model (DEM).

Advanced techniques based on simultaneous processing of series of SAR acquisitions make it possible to mitigate problems of conventional InSAR. One category of algorithms for processing multiple acquisitions is the so-called Persistent Scatterers (PS-InSAR) methods. The main principle of these methods is in simultaneous analysis of a number of pair interferograms, considering only pixels with some "stable behaviour" called "Persistent (or sometimes Permanent) Scatterers" (PS). The necessary procedure for the PS-InSAR methods is coregistration of all the images from the set with one so-called "master" image. The main difference between the existing PS-InSAR methods is in mathematical definition of the PSs. Initially techniques of PS identification mostly relied on analysis of amplitude values of pixels in a series of interferograms (e.g. [1]-[6]). These PS-InSAR methods are especially efficient in urban areas where man-made structures increase the likelihood of finding stable scatterers. Although density of PS pixels identified in natural terrains is much lower there exist a number of examples of successful implementation of this technique for landslide monitoring (e.g. [7]-[12]). Some of the above referred techniques have been further developed to improve identification of PS in non-urban areas (e.g. [13]).

For PS-InSAR processing we used the StaMPS software (Stanford Method for Persistent Scatterers) [14, 15, 16], which uses spatial correlation of interferogram phase to find pixels with low-phase variance in all terrains, with or without buildings. The StaMPS shows good results for alternating urban and rural areas which is rather common for the Black Sea Coast of the Great Caucasus. We incorporated the ALOS (wavelength 23.5 cm, ascending orbit), Envisat (wavelength 5.6 cm, descending orbit) and TerraSAR-X (wavelength 3.1 cm, ascending orbit) acquisitions covering successively five year time period since January 2007 to September 2012.

At first we describe the study area, and satellite data involved. Then we present results of calculations of displacements over the study area. Areas showing significant displacement rates are compared to the landslide activity map based on geological field data. For the two landslides situated in the Baranovka and Mamaika villages we present time series for all the data sets and analyse variations of the surface displacement in time. Our research proved the efficiency of active landslides location in the Great Caucasus and monitoring their activity incorporating acquisitions from satellites imaging in different frequency bands using the StaMPS PS-INSAR method.

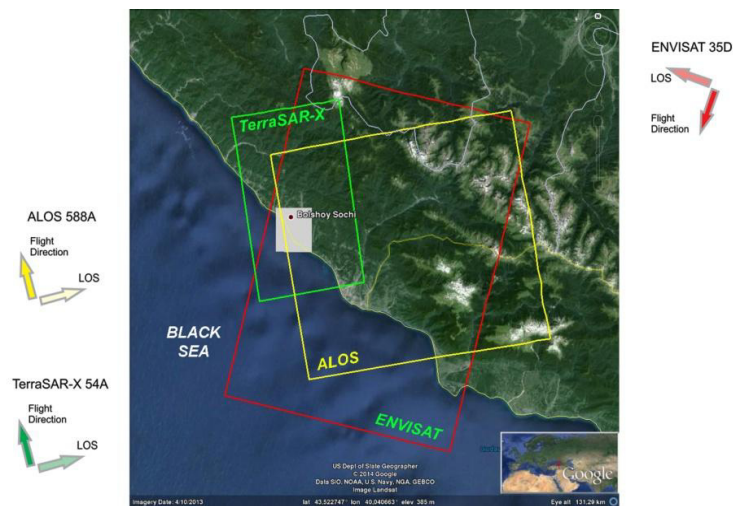


Fig. 1. The study area - Bolshoy Sochi (the white shaded rectangle); the geometry and frames of the SAR acquisitions: yellow - the ALOS track 588A; red - the Envisat track 35D; green - the TerraSAR-X-track 54A.

## 2. Study area and satellite data

The study area is located on the Black Sea coast of the Great Caucasus in the Bolshoy (Big) Sochi region (Fig. 1). It covers a large territory around the Sochi city which is related to the Sochi-2014 Olympic Games Facilities. To investigate the landslide activity in the study area we incorporated 3 sets of images which cover the time period from January 2007 to September 2012 with almost no time gaps. These sets are as follows:

- 17 ALOS images from 22.01.2007 to 17.09.2010, track 588A (ascending orbit)
- 13 Envisat images from 29.11.2010 to 23.03.2012, track 35D (descending orbit) - acquired after the orbit manoeuvre in October 2010
- 17 TerraSAR-X images from 24.12.2011 to 13.09.2012, track 54 A (ascending orbit)

The frames and geometry of acquisitions are shown in Fig. 1. Dates of acquisitions and perpendicular baseline values in relation to the corresponding master-images are presented in Fig. 2 a, b, c.

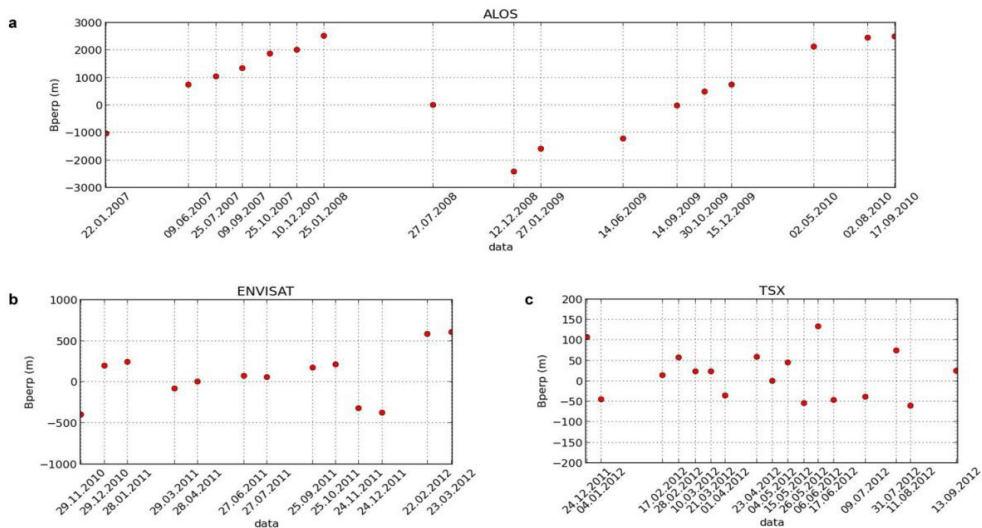


Fig.2. The dates of acquisitions and perpendicular baseline values related to the master images for (a) ALOS 588A (the master image-27.07.2008), (b) Envisat 35D (the master image-28.04.2011) and (c) TerraSAR-X (the master image-04.05.2012)

## 3. Results

Using the StaMPS software for all the above mentioned sets of images we managed to identify persistent scatterers with the density of more than 350PS/km. For all these PS we calculated ground displacements in the line of site (LOS) direction of the satellites. The results of calculations of the ground displacements overlapped on the map of recent landslide activity based on the ground data [17] are presented in Fig.3. As the PS density is rather high, thus, to make the ground data map visible we displayed only the PS having average displacement rates in the line of site direction of the satellite ( $V_{LOS}$ ) more than 15mm/year.

For the two landslides for which considerable surface displacements were found during the time of acquisitions (the Baranovka and Mamaika villages marked as 1 and 2 in Fig.3) we present distributions of all PS identified for the data sets from all the three satellites (Fig.4 and 5).



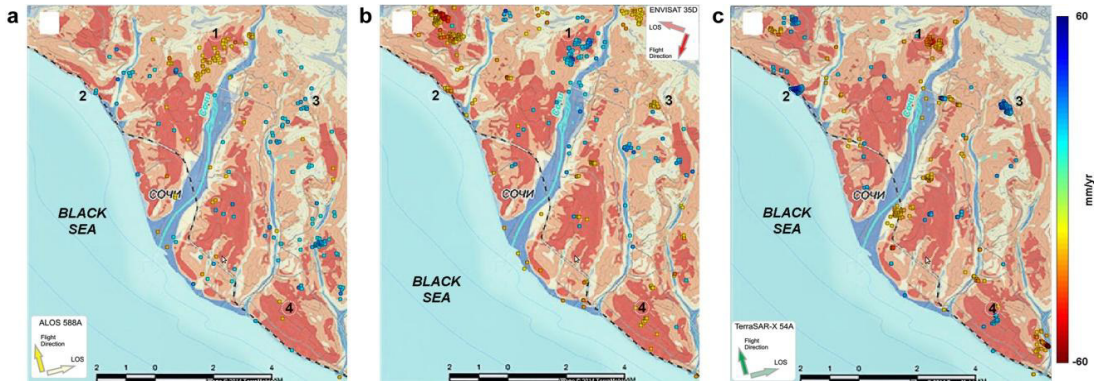


Fig. 3. The distribution of the PS (circles) identified using the StaMPS PS-InSAR method for which average displacement rate in the LOS direction ( $V_{LOS}$ ) exceed 15mm/year for the (a) ALOS 588A, (b) ENVISAT 35D and (c) TerraSAR-X 54A image sets. Background - the map of landslide activity for the Bolshoy Sochi area based on the ground data [17]. Intensity of colour on the map corresponds to landslide activity. Colours of the PS: blue - towards satellite; red - away from satellite. The landslides where considerable movements were fixed during the period of the acquisitions are numbered as follows: 1-Baranovka ; 2- Mamaika;3-Verkhni Yar;4-Bytkha.

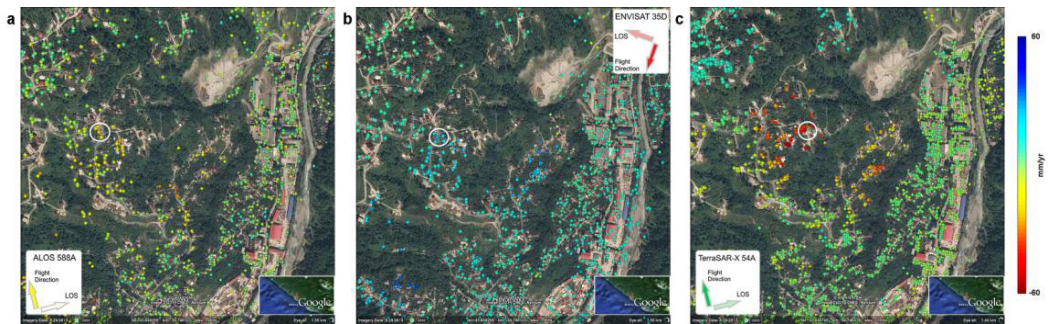


Fig.4. The PS distribution in the Baranovka landslide area for the ALOS-track 588A (a), Envisat-track 35D (b) and TerraSAR-X-track 54A (c) data sets on the Google Earth map. Colours of the PS are proportional to values of  $V_{LOS}$  and correspond to the direction of their movements: blue-towards the satellite, red-away from the satellite, green-negligibly small values. White circles bound the PSs which LOS displacements are typical for the landslide slope.



Fig.5. The PS distribution in the Mamaika landslide area. The rest figure captions are the same as in Fig.4.

#### 4. Discussion

Analysis of the distribution of the PSs with comparatively high LOS average displacement rate values ( $V_{LOS} > 15$  mm/year) for the whole study area (Fig.3) shows that clusters of these PSs are situated within areas of high landslide activity mapped by geological field study. In particular, PS clusters indicate the areas of recent landslide activity: Baranovka (1), Mamaika (2), Verkhni Yar (3); Bytkha (4) where noticeable movements were fixed on the ground during the time of acquisitions.

The LOS projection of the displacement vector for almost all the landslide slopes has opposite sign for the ascending tracks of the ALOS and TerraSAR-X satellites in comparison to the descending track of the Envisat (see PS colours in Fig. 3,4,5). The quantity of the PSs in all the three data sets is different. This can be explained as follows. Steep forested slopes widely spread in the study area are not favourable for the SAR interferometry. Only few PSs could be identified there even using the long wavelength ALOS data. At the same time high resolution of the TerraSAR-X satellite makes it possible to identify much more PSs in urban territories of the study area than other satellites do. Moreover, the urban territories of the study area had been an area of extensive construction activity and many new scatterers appeared there in the last few years. Besides the set of the TerraSAR-X images covers shorter time interval, is denser in time and does not contain considerable time gaps. All this explains why the quantity of the PSs identified using the TerraSAR-X data far exceeds those of the other satellites.

When interpreting the displacement maps of the study area based on the SAR data (Fig. 3,4,5) it is also important to bear in mind that not all slopes can be "seen" by SAR as there exist zones of shade and overlapping. In addition exposition of landslide slopes is also important as movements of scatterers in the direction close to the satellite track can hardly be fixed by the SAR interferometry. Thus, to enhance reliability of localization of active landslides it is worth using SAR images acquired for the same periods of time, in different frequency bands, and from both ascending and descending tracks.

Direct comparison of the calculated LOS displacement rates from the three discussed data sets is impossible because geometry of the acquisitions for these sets is different. Assuming that movements are oriented down the landslide slope it can be shown that:

$$u_{LOS} = -u \cdot (\sin \alpha \cdot \cos \theta + \cos \alpha \cdot \sin \theta \cdot \sin(\gamma - \beta)), \quad (1)$$

where  $u_{LOS}$  is the LOS displacements, and  $u$  is the module of the displacement vector. The other notations are explained in Fig.6. The same equation holds for average displacement rates  $V_{LOS}$  and  $V$  instead of  $u_{LOS}$  and  $u$ . Characteristic  $\beta$  and  $\theta$  values for different satellites are presented in Table 1.

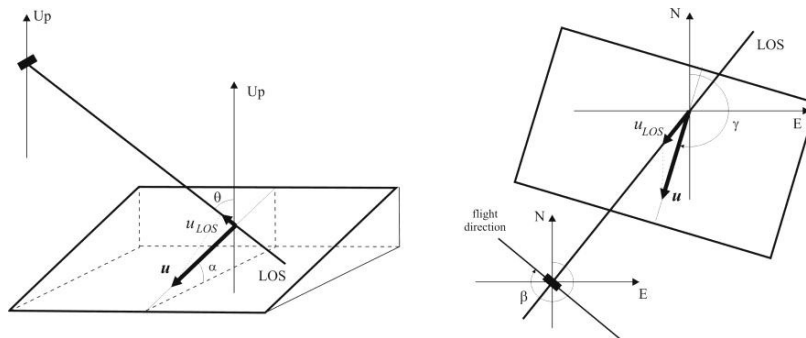


Fig.6. Geometry of satellite acquisition in 3D (left) and in the top view (right). Satellite image geometry:  $\theta$  - incidence angle;  $\beta$  - satellite heading. Landslide movement geometry:  $u$  - displacement vector which dip is  $\alpha$  and azimuth is  $\gamma$ ;  $u_{LOS}$  - its LOS projection.

Table 1. Characteristic values of heading  $\beta$  and incidence angle  $\theta$  for the ALOS, ENVISAT и TerraSAR-X.

Satellite	heading, $\beta$ , (°)	incidence angle, $\theta$ , (°)
ALOS, track 588A (ascending orbit)	346	38
ENVISAT, track 35D (descending orbit)	195	42
TerraSAR-X, 54 (ascending orbit)	350	45

Let us now consider displacement rates for the landslides in the Baranovka and Mamayka villages (number 1 and 2 in Fig. 3) in more details.

#### 4.1. The Baranovka landslide



Fig. 7. Damage in the Baranovka village after the landslide movement on 23-24 January 2012.

The Baranovka landslide is rather big: the estimated surface coverage is 8 ha and its thickness is about 30m. The intensive movements were fixed there at night on 23-24 January 2012. Presumably activation of this landslide was provoked by improper constructive works. Fortunately, there were no fatalities but 35 houses were damaged and 170 people resettled. According to local people, surface movements in this region became visible in December 2011 when cracks on the walls of the houses appeared, tubes and widow glasses were ruptured. The pictures of damage in the Baranovka village are presented in Fig. 7.

Analyzing the average displacement rates for the PSs identified from all the data sets (Fig. 4 a,b,c) one can point out that movements of the Baranovka landslide are most pronounced in the results of PS-InSAR processing of the TerraSAR-X data (Fig. 4c). The explanation is that the ALOS acquisitions completed before the landslide collapse and only two Envisat images were acquired after it. As the acquisitions cover different time periods we plotted time series for all the data sets (Fig. 8 a,b,c). TS for each satellite data set were averaged for PSs in the areas with typical displacement rates for the landslide (shown by white circles in Fig.4). The Baranovka village is situated in the region with rather complicated topography where the slope dip ( $\alpha$ ) and azimuth of land sliding ( $\gamma$ ) vary. The areas with typical landslide displacement rates found from the ALOS and Envisat data sets (Fig.4 a,b) are located on the slope facing to the west which dip does not exceed  $5^\circ$ . The PSs with typical movement rate found from the TerraSAR-X data are located on the much steeper slope exposed to the south-east (Fig. 4 c). As a result, for the ALOS и ENVISAT data sets we assigned  $\alpha=5^\circ$  and  $\gamma=90^\circ$ , while for the TerraSAR-X:  $\alpha=18^\circ$  and  $\gamma=165^\circ$ .



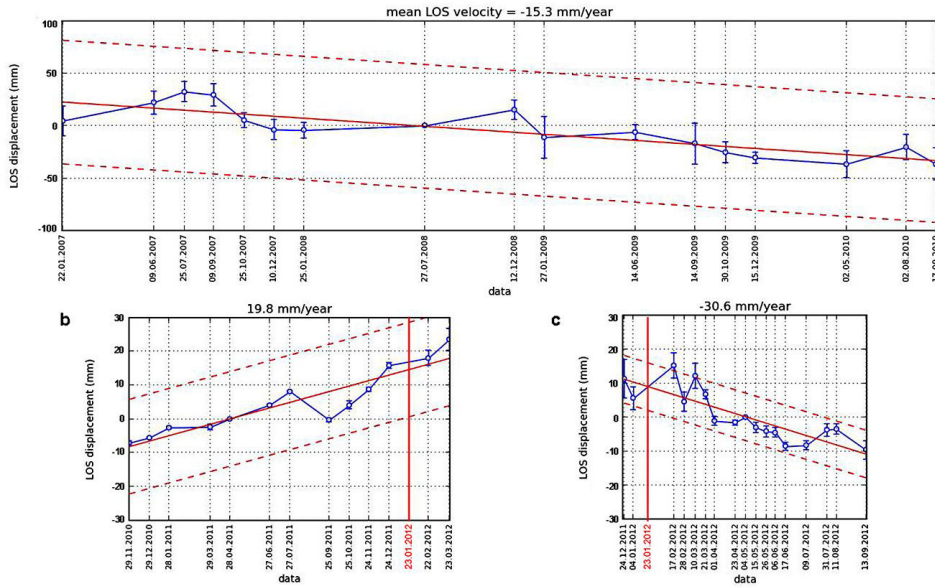


Fig. 8. The time series for the PSs in the Baranovka landslide area for the ALOS-track 588A (a), Envisat-track 35D (b) and TerraSAR-X track 54A (c), averaged for the group of the PSs located in areas shown by white circles on Fig. 4. The LOS displacements for the Envisat ascending track have the opposite sign in relation to the ones for the ALOS and TerraSAR-X because of the acquisition geometry.

Time series for the ALOS data from 22.01.2007 to 17.09.2010 (Fig. 8 a) are rather smooth and show sliding at nearly constant LOS displacement rate  $V_{LOS}=15.3$  mm/year. Accounting for the equation (1), Table 1 and assuming  $\alpha=5^\circ$ ,  $\gamma=90^\circ$  this corresponds to the displacement rate in the direction down the slope equal to  $V = 25$  mm/year. One period of acceleration between 25.07.2007 and 10.12.2007 can be noticed. The displacement for these five months came up to  $u_{LOS}=30$  mm ( $u = 45$  mm). Unfortunately we did not find ground data on the landslide activity during this time period. The time series for the Envisat data can be subdivided into the two intervals: from 29.11.2010 to 27.07.2011 and from 25.09.2011 to 23.03.2012 with the  $V_{LOS}$  values 20 mm/year ( $V\approx 35$  mm/year) and 50 mm/year ( $V\approx 85$  mm/year) correspondingly. This suggests that the acceleration of the landslide movements occurred there since autumn 2011. High amplitude displacements of 22-23 January 2012 are not manifested in the Envisat time series although some acceleration can be seen during 22.02.2012-23.03.2012.

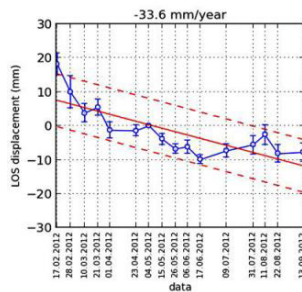


Fig. 9. The time series for the TerraSAR-X data for period 17.02.2012 - 13.09.2012 after the landslide event 22-23 January 2012 (averaged for the group of the PS located in the area bounded by the white circle in Fig.4c).

The TS based on the TerraSAR-X data appeared to be the most informative. It is difficult to estimate velocities of movements during the event of 22-23 January 2012 because estimated displacement rates may contain unwrapping

errors for the interval 24.12.2011 - 10.03.2012. To investigate movements of the landslide during its activation we carried out additional calculations for the shorter period 17.02.2012-13.09.2012. The corresponding time series are presented in Fig. 9.

The TS in Fig. 9 shows faster movements for the period 17.02.2012 - 10.03.2012 when  $V_{LOS}$  exceeded 30 mm/month ( $V \approx 120$  mm/month). Then movements slowed down and since 06.06.2012 they stabilized becoming smaller than 2-3 mm/month ( $V \approx 10$  mm/month), which is consistent with the ground observations.

To estimate values of the displacements during the event of 22-23 January 2012 we also analyzed two TerraSAR-X differential interferograms 17.02.2012 -28.02.2012 (Fig. 10a) and 28.02.2012 - 21.03.2012 (Fig. 10b).

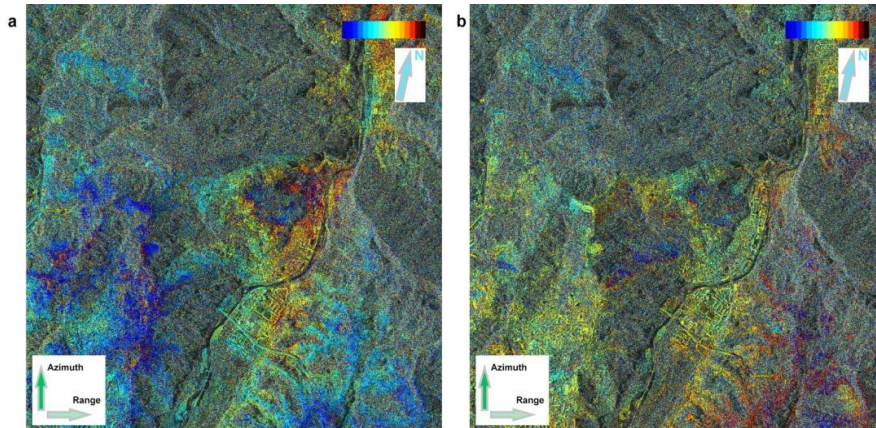


Fig.10. The TerraSAR-X (track 54A) interferograms for the area of the Baranovka landslide (topography effects subtracted): (a) - 17.02.2012 - 28.02.2012 and (b) - 28.02.2012 - 21.03.2012

On the left interferogram almost full fringe is evident. That means that during 11 days between 17.02.2012 and 28.02.2012 the displacements in the LOS direction  $u_{LOS}$  exceeded 10-12mm ( $u > 40$  mm). The right interferogram is not so clear but anyway at least half of the fringe can be seen. That corresponds to displacements  $u_{LOS} \approx 5-7$  mm ( $u \approx 25$  mm). That is in agreement with time series discussed above and proves the reliability of unwrapping when plotting the displacement maps.

It is worth noting that in the areas where the TerraSAR-X data from ascending orbit showed high LOS displacement rates (one of them is marked by white circle in Fig. 4e), only few PSs were identified using the ENVISAT data from descending orbit. The possible explanation is in acquisition geometry. For the slopes exposed to the south-east the Envisat data from descending orbits are more sensitive to small displacements in the LOS direction. On the contrary strong displacements leading to the loss of coherence between images from descending tracks can be still seen from the ascending ones.

#### 4.2. The Mamaika landslide

Analyzing the PS distribution for all the data sets for the sequential periods of time (Fig. 5 a,b,c) one can conclude that during 5 years of investigations the area involved in the Mamaika landslide increased. To investigate the displacement rates we again plotted the time series for each satellite averaging the TS for all the PSs in the areas where LOS displacements seems to be typical for the landslide slope (marked by the white circles in Fig. 5 a,b,c).

For the time period 22.01.2007 - 17.09.2010 LOS displacement rates were estimated as  $V_{LOS} = 14.9$  mm/year (the ALOS data), for the period 24.12.2011 - 13.09.2012 as  $V_{LOS} = 54.2$  mm/year (the TerraSAR-X data). The Envisat data (the period 29.11.2010 - 23.03.2012) showed much slower LOS displacement rates  $V_{LOS} = 15.8$  mm/year due to different acquisition geometry. To investigate  $V_{LOS}$  variation in time, we estimated displacement rates in the down the landslide slope direction for all data sets using formula (1) and Table 1. The main part of the Mamaika landslide



moves to the south-west with azimuth  $\gamma = 230^\circ$  and dip  $\alpha = 11^\circ$ . Thus, the estimated values of the average displacement rates down the slope for the ALOS (22.01.2007 - 17.09.2010), ENVISAT (29.11.2010 - 23.03.2012) and TerraSAR-X (24.12.2011 - 13.09.2012) are correspondingly 30, 35 and 75 mm/year. This allows us to make a conclusion about possible acceleration of the Mamaika landslide movements during the period of observations.

More detailed consideration of the PS-InSAR monitoring of the surface displacements of the Mamaika landslide can be found in [18], [19].

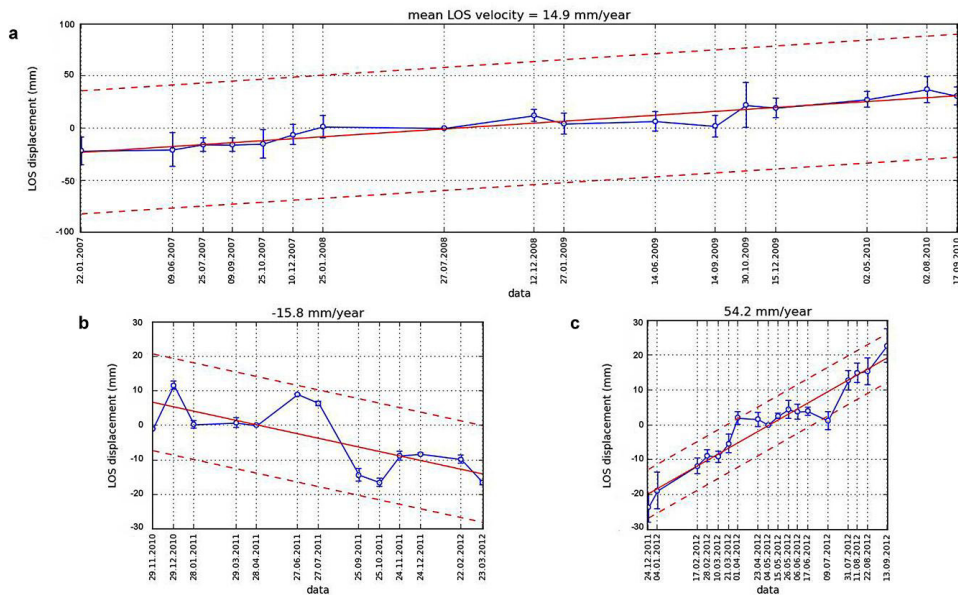


Fig. 11. The time series for the Mamaika landslide for ALOS-track 588A(a), Envisat-track 35D (b) and TerraSAR-X-track 54A (c) averaged for the group of the PS located in the area bounded by the white circles in Fig.5).

## 5. Conclusion

Application of the StaMPS PS-InSAR technique permitted us to locate the main landslides in the area of the Bolshoy Sochi where active landslide movements were revealed using ground data. Investigation of the time series for the Baranovka and Mamaika landslides made it possible to determine periods of their activity and relative stability and compare this periods with ground observations.

Images from the L-band, C-band and X-band satellites can be used to monitor displacements of the landslides in the Black Sea coast of the Great Caucasus. To enhance reliability of the monitoring the comparative analysis of results obtained from the satellites with different wavelengths and from both the ascending and descending tracks is preferable.

Obtained results demonstrate that PS-InSAR is an efficient tool to locate landslides and monitor their displacements at the Black Sea coast and in the Great Caucasus Mountains. As landslides are numerous in this region these methods could contribute to landslide risk assessment and mitigation.

## Acknowledgements

Authors acknowledge the European Space Agency ESA (project C1-7991), the Japanese Space Agency JAXA and the Deutsches Zentrum für Luft- und Raumfahrt DLR (project LAN1247) who kindly supplied us with the SAR data for this study.

## References

- [1] Ferretti, A., Prati, C. & Rocca, F. Nonlinear subsidence rate estimation using Permanent Scatterers in Differential SAR Interferometry. *IEEE Trans. Geosci. Remote Sens.* 2000;38(5) :2202-2212.
- [2] Ferretti, A., Prati, C. & Rocca, F. Permanent Scatterers in SAR Interferometry. *IEEE Trans. Geosci. Remote Sens.* 2001;39(1): 8-20.
- [3] Colesanti, C., Ferretti, A., Prati, C. & Rocca, F. . Monitoring landslides and tectonic motion with the Permanent Scatterers technique. *Engineering Geology* 2003;68:1–14.
- [4] Adam N., Parizzi A., Eineder M. & Crosetto M. Practical persistent scatterer processing validation in the course of the TerraFirma project. *Journal of Applied Geophysics* 2009;69:5965.
- [5] Crosetto, M., Castillo, M. & Arbiol, R. Urban subsidence monitoring using radar interferometry: Algorithms and validation. *Photogrammetric Engineering and Remote Sensing* 2003;69(7):775–783.
- [6] Lyons S. & Sandwell D. Fault creep along the southern San Andreas from interferometric synthetic aperture radar, permanent scatterers, and stacking. *JGR* 2003;108 (B1): doi:10.1029/2002JB001831.
- [7] Kimura, H. & Yamaguchi Y. Detection of landslide areas using satellite radar interferometry, *Photogrammetric Engineering & Remote Sensing* 2000;66(3):337–344.
- [8] Colesanti C. & Wasowski J. Investigating landslides with space-borne Synthetic Aperture Radar (SAR) Interferometry. *Engineering Geology* 2006;88:173–199.
- [9] Meisina C., Zucca F., Conconi F., Verri F., Fossati D., Ceriani M. & Allievi J. Use of Permanent Scatterers technique for large-scale mass movement investigation. *Quaternary International* 2007;171–172:90-107.
- [10] Farina P., Colombo D., Fumagalli A., Marks F. & Moretti S. Permanent Scatterers for landslide investigations: outcomes from the ESA-SLAM project. *Engineering Geology* 2006;88:200-217.
- [11] Farina P., Casagli N. & Ferretti A. (2008). Radar-interpretation of InSAR measurements for landslide investigations in civil protection practices. *First North American Landslide Conference*, June 3-8, 2007. Vail, Colorado, 272-283.
- [12] Brugioni M., Mazzanti B., Montini G. & Sulli L. (2011). Use of SAR interferometry for landslide analysis in the Arno river basin. *Proceedings of the Second World Landslide Forum – 3-7 October 2011, Rome, Italy.*
- [13] Ferretti, A., Fumagalli, A., Novati, F., Prati, C., Rocca, F., Rucci, A. A new algorithm for processing interferometric data-stacks: SqueeSAR. *IEEE Transactions on Geoscience and Remote Sensing* 2011; <http://dx.doi.org/10.1109/TGRS.2011.2124465>
- [14] Hooper, A., H. Zebker, P. Segall, & B. Kampes. A New Method for Measuring Deformation on Volcanoes and Other Natural Terrains Using InSAR Persistent Scatterers. *Geophys. Res. Letters* 2004;31: L23611, doi:10.1029/2004GL021737.
- [15] Hooper, A., P. Segall, and H. Zebker, Persistent Scatterer InSAR for Crustal Deformation Analysis, with Application to Volcán Alcedo, Galápagos, *J. Geophys. Res.* 2007;112, B07407, doi:10.1029/2006JB004763.
- [16] Hooper A., Spaans K., Bekaert D., Cuenca M.C., Arian M. & Oyen A. *StaMPS/MTI Manual*, Delft Institute of Earth Observation and Space Systems Delft University of Technology, Kluyverweg 1, 2629 HS, Delft, The Netherlands 2010; ([http://radar.tudelft.nl/~ahooper/stamps/StaMPS\\_Manual\\_v3.2.pdf](http://radar.tudelft.nl/~ahooper/stamps/StaMPS_Manual_v3.2.pdf)).
- [17] [http://geomonitoring.ru/Sochi/gal\\_new/%D0%93%D0%98%D0%A1-%D0%B0%D1%82%D0%BB%D0%B0%D1%81%20%D0%BA%D0%B0%D1%80%D1%82%20%D0%A1%D0%BE%D1%87%D0%B8%D1%81%D0%BA%D0%BE%D0%B3%D0%BE%20%D0%BF%D0%BE%D0%BB%D0%B8%D0%B3%D0%BE%D0%BD%D0%B0/sochi\\_2014.html](http://geomonitoring.ru/Sochi/gal_new/%D0%93%D0%98%D0%A1-%D0%B0%D1%82%D0%BB%D0%B0%D1%81%20%D0%BA%D0%B0%D1%80%D1%82%20%D0%A1%D0%BE%D1%87%D0%B8%D1%81%D0%BA%D0%BE%D0%B3%D0%BE%20%D0%BF%D0%BE%D0%BB%D0%B8%D0%B3%D0%BE%D0%BD%D0%B0/sochi_2014.html)
- [18] Mikhailov V., Kiseleva E., Smolyaninova E, Golubev V., Dmitriev P., Isaev Yu., Dorokhin K., Hooper A., Samiei-Esfahany S., Hanssen R. PS-INSAR monitoring of landslides in the Great Caucasus, Russia, using ENVISAT, ALOS and TerraSAR-X SAR images. *Proceedings of ESA Living Planet Symposium*, 9 - 13 September, 2013, Edinburgh, UK.
- [19] Mikhailov V. O., Kiseleva E. A., Smol'yaninova E. I., Dmitriev P. N., Golubev V. I., Isaev Yu. S., Dorokhin K. A., Timoshkina E. P., and Khairetdinov S. A. Some Problems of Landslide Monitoring Using Satellite Radar Imagery with Different Wavelength: Case Study of Two Landslides in the Region of Big Sochi. *Izvestiya, Physics of the Solid Earth*, 2014;50 (4):1-11.